ELSEVIER

www.elsevier.nl/locate/jorganchem

Journal of Organometallic Chemistry 587 (1999) 207–214

Journal of Organometallic Chemistry

Synthesis and X-ray crystal structures of mixed sandwich Group 8 cyclopentadienyl complexes containing crown trithioether ligands

Gregory J. Grant [a,*], Terese Salupo-Bryant [a], Lisa A. Holt [a], Denise Y. Morrissey [a], Mary Jo Gray [a], Jeffrey D. Zubkowski [b], Edward J. Valente [c], Larry F. Mehne [d]

[a] *Department of Chemistry, The University of Tennessee, Chattanooga, TN 37403, USA*
[b] *Department of Chemistry, Jackson State University, Jackson, MS 39217, USA*
[c] *Department of Chemistry, Mississippi College, Clinton, MS 39058, USA*
[d] *Department of Chemistry, Covenant College, Lookout Mountain, GA 30750, USA*

Received 18 February 1999

Abstract

The syntheses and characterization of three new mixed sandwich complexes involving crown thioether ligands and Group 8 metal ions are reported. These complexes are: $[Ru(C_5H_5)(9S3)]PF_6$ (**1**), $[Ru(C_5H_5)(10S3)]PF_6$ (**2**) and $[Fe(C_5H_5)(10S3)]PF_6$ (**3**), where 9S3 = 1,4,7-trithiacyclononane and 10S3 = 1,4,7-trithiacyclodecane. All three complexes have been characterized by single-crystal X-ray crystallography, and all structures show an octahedral metal center with facially coordinated carbocyclic and macrocyclic ligands. The average M–S bond lengths in **1**, **2** and **3** are 2.289(2), 2.331(2) and 2.1823(7) Å, respectively, and these are shorter than the M–S bond lengths in the corresponding bis 9S3 and 10S3 complexes. We propose that this distance decrease is caused by enhanced metal–thioether π bonding due to the strong σ-donating ability of the Cp ligand. All structures are confirmed in solution via ^{1}H- and ^{13}C-NMR spectroscopy. Cyclic voltammetric studies on the three heteroleptic complexes show $E_{1/2}$ values that are intermediate between those of the corresponding homoleptic hexakis(thioether) complexes and metallocenes. This electrochemical behavior is also consistent with the relative σ-donating and π-accepting abilities of the Cp and trithioether ligands.

Keywords: Cyclopentadienyl complexes; Ruthenium complexes; Thioethers; Trithiacyclononane

1. Introduction

The past decade has witnessed an intense period of research into the coordination chemistry of crown thioether ligands, with several groups examining the complexation characteristics of ligands such as 1,4,7-trithiacyclononane (9S3) [1–5]. Ligands such as 9S3 have also been shown to form stable transition metal sandwich compounds, and the coordination chemistry of these ligands has received a good deal of attention because of the unusual stereochemical, spectroscopic, and electrochemical properties exhibited by the crown thioether complexes [6–13]. Furthermore, the examination of the organometallic chemistry of 9S3 has recently begun, and the past few years have seen a number of research groups active in this particular area of thioether coordination chemistry [14–24]. Unusual properties exhibited by organometallic complexes of 9S3 include reaction chemistry such as double deprotonation and subsequent opening of the thioether ring [25], fluxional behavior of the 9S3 ligand, and formation of mixed thioether sandwich complexes [21]. The 9S3 ligand can be compared to η^5-cyclopentadienide (Cp), η^6-arene, and κ^3-$HB(pz)_3$ (pz = pyrazol-1-yl) ligands in that all are six-electron donors that occupy three facially coordinating sites. A report of a Ru(II) complex containing mixed sandwich carborane/9S3 complexes has also recently appeared [17]. The formation of tricarbonyl Mo(0) and W(0) complexes with 9S3 and related ligands ('piano stool' complexes) is illustrative of the general π-acidity exhibited by thioethers [1–5,26–28].

Complexes involving 1,4,7-trithiacyclodecane (10S3), another six-electron facially coordinating thioether lig-

* Corresponding author.

0022-328X/99/$ - see front matter
PII: S0022-328X(99)00322-8

and, were also prepared. Conformational distinctions between 9S3 and 10S3 must be noted when examining the complexation behavior of these ligands towards transition metals. The conformation of the free 9S3 ligand has been shown to be the one in which all three sulfur atoms are *endodentate*, and thus it requires no reorganization for facial coordination to a metal center [29]. The possible conformations of the 10S3 ligand have been previously described, only four of which are oriented for facial tridentate coordination [6]. Molecular mechanics calculations have shown that the lowest-energy conformations of the 10S3 do not involve an exclusive *endodentate* conformation. Rather, in complexes such as $[Fe(10S3)_2]^{2+}$, the ligand must assume a higher-energy *endodentate* conformation in order to coordinate via all three sulfur atoms.

Schröder and co-workers have reported the synthesis and characterization of the mixed sandwich complex $[Fe(Cp)(9S3)]^+$ [21]. We have prepared the 10S3 analog as well as the related mixed-sandwich ruthenium(II) complexes containing 9S3 and 10S3. Ruthenium(II), in particular, has been shown to have a strong affinity for crown thioether ligands [10–12]. The complexes $[M(Cp)(L)]^+$ (M = Fe, Ru; L = 9S3, 10S3) possess heteroleptic ligand environments that are intermediate between the corresponding metallocenes and hexakis(thioether) complexes. Therefore, these mixed sandwich complexes should exhibit structural, spectroscopic, and electrochemical properties intermediate between those of the two types of homoleptic sandwich complexes.

2. Results and discussion

2.1. Syntheses and spectroscopic data

The three complexes are readily prepared by the substitution of the appropriate crown thioether ligand for coordinated carbonyl and iodide ligands in the case of Fe or for phosphine and chloride ligands for Ru.

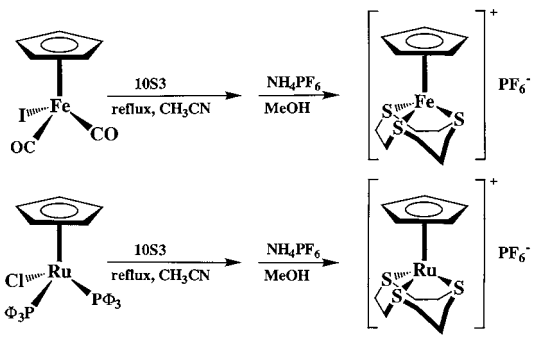

Scheme 1.

The syntheses of the two 10S3 complexes are illustrated in Scheme 1.

The structural assignments are supported by the analytical, infrared, and ^1H- and $^{13}C\{^1H\}$-NMR data, in particular, which exhibit resonances exclusively due to both the Cp ligand and the coordinated trithioether. The ABCD pattern observed for the methylene proton resonances in $[Ru(Cp)(9S3)]^+$ was also seen in the corresponding Fe complex [21]. Also, the four-line pattern of the carbon resonances in both 10S3 complexes is in the anticipated 2:2:2:1 ratio. The electronic spectroscopic data show stronger ligand fields in the Ru complexes relative to the Fe complexes and also stronger ligand fields in the 9S3 complexes relative to the 10S3 analogs. These trends are expected based upon previous observations of hexakis(thioether) complexes of Fe and Ru [6,8,10,12].

Due to enhanced π bonding between the softer Ru ion and the thioether, the substitution of iron by ruthenium results in a small downfield ^{13}C-NMR shift for both the cyclopentadienyl resonance and the thioether resonances. This π bonding between the metal and the crown thioether also results in a downfield shift of several ppm for the thioether resonances compared with the related bis complexes of 9S3 and 10S3. However, the identity of thioether ligand for the ruthenium complexes does not appear to influence the chemical shift of the Cp resonance.

2.2. Structural studies

The structures of $[Ru(Cp)(9S3)](PF_6)$ (**1**), $[Ru(Cp)(10S3)](PF_6)$ (**2**), and $[Fe(Cp)(10S3)](PF_6)$ (**3**) were determined by single-crystal X-ray diffraction. A summary of crystallographic data for the three structures is reported in Table 1, and structural perspectives are shown in Figs. 1–3. All three complexes crystallize in the same $P2_1/m$ space group. Both the trithioether ligands and Cp coordinate facially to the metal ion to form a six coordinate complex.

The crystal structures of both ruthenium complexes contain disorder in the thioether ring. For **1** the disorder model contains two $[Ru(Cp)(9S3)]^+$ cations in equal amounts. The two orientations found for 9S3 are mirror related and defined by a mirror plane perpendicular to the plane containing the sulfur atoms. This results in different orientations of the ethylene chelate rings. Similar disorder behavior has also been observed in the crystal structure of $[Ir(9S3)(cod)]^+$ in which two equally populated conformations of 9S3 were found [20]. In contrast, the disorder in the structure of $[Fe(Cp)(9S3)]^+$ is two equally populated orientations of the cyclopentadienyl ring [21]. For **2** the disorder model contains three cation conformations involving the orientation of the propyl segment. The first conformer is the one pictured in Fig. 2 and has S(1) and C(7) on the

Table 1
Crystallographic data and structural refinement for [CpRu(9S3)][PF_6] (**1**), [CpRu(10S3)][PF_6] (**2**) and [CpFe(10S3)][PF_6] (**3**)

	1	**2**	**3**
Chemical formula	$C_{11}H_{17}F_6PRuS_3$	$C_{12}H_{19}F_6PRuS_3$	$C_{12}H_{19}F_6FePS_3$
Formula weight (a.m.u.)	491.47	505.49	460.27
Color	Yellow	Yellow	Red
Crystal size (mm)	$0.07\times0.05\times0.10$	$0.05\times0.05\times0.03$	$0.50\times0.20\times0.10$
Crystal system	Monoclinic	Monoclinic	Monoclinic
Space group	$P2_1/m$	$P2_1/m$	$P2_1/m$
a (Å)	7.2380(10)	7.366(2)	7.767(2)
b (Å)	13.353(3)	14.264(4)	13.905(3)
c (Å)	8.139(2)	8.282(2)	7.982(2)
β (°)	97.85(3)	98.60	99.12(2)
V (Å^3)	779.3(3)	860.4(4)	851.2(4)
$D_{calc.}$ (g cm^{-3})	2.095	1.951	1.796
Z	2	2	2
μ (Mo–K_α) mm^{-1}	1.564	1.419	1.399
F(000)	488	504	468
Temperature (K)	293	293	293
λ (Mo–K_α) (Å)	0.71073	0.71073	0.71073
θ range for data collection (°)	2.53–28.00	2.49–32.51	2.58–59.99
Index ranges	$0\le h\le9$, $0\le k\le17$, $-10\le l\le10$	$0\le h\le11$, $0\le k\le21$, $-12\le l\le12$	$0\le h\le10$, $0\le k\le19$, $-11\le l\le11$
Reflections collected	2028	3499	3595
Independent reflections	1894 [$R_{int}=0.0765$]	3213 [$R_{int}=0.0315$]	2575 [$R_{int}=0.0131$]
Refinement method	Full-matrix least-squares on F^2	Full-matrix least-squares on F^2	Full-matrix least-squares on F^2
Data/restraints/parameters	1894/0/143	3213/0/131	2575/0/112
Final R indices [$I>2\sigma(I)$]	$R_1=0.0298$, $wR^2=0.0791$	$R_1=0.0526$, $wR^2=0.1362$	$R_1=0.0394$, $wR^2=0.1149$
R indices (all data) [a]	$R_1=0.0335$, $wR^2=0.0928$	$R_1=0.0714$, $wR^2=0.1412$	$R_1=0.0493$, $wR^2=0.1149$
Goodness-of-fit [b] on F^2	1.235	0.953	0.924
Largest diff. peak and hole (e A^{-3})	1.061 and −0.846	2.517 and −1.621	0.707 and −0.475

[a] $R_1=\Sigma\||F_o|-|F_c|\|=\Sigma|F_o|$, $wR^2=[\Sigma\, w(F_o^2-F_c^2)^2=\Sigma(wF_o^4)]^{1/2}$.
[b] Goodness-of-fit $=[\Sigma\, w(|F_o|-|F_c|)^2=(n_o-n_v)]^{1/2}$ where n_o = number of observations, n_v = number of parameters and w = weights. Weight $=1/\sigma^2(F_o^2)+(0.0679*P)^2+0*P$, where $P=(\max(F_o^2,0)=2*F_c^2)/3$.

mirror plane of the molecule. The second and third conformers are mirror images of each other. The site occupation factors for the three conformations are 50, 25 and 25%, respectively. This disorder is absent in our previously published structure of $[Ru(10S3)_2]^{2+}$ [12] as well as in the structure of $[Fe(Cp)(10S3)]^+$ (see Fig. 3) presented in this report, but it has been observed in the reported structures of $[Ni(10S3)_2]^{2+}$ and $[Co(10S3)_2]^{2+}$ [13].

The 10S3 ligand adopts the [2323] conformation in the crystal structure of **3**, the same conformation found previously in several structures involving homoleptic complexes of this ligand [6,9,12]. This conformation necessarily places the six-membered chelate ring in a chair form. As expected, the internal S–Fe–S angles of the five-membered chelate rings are smaller than those of the six-membered chelate rings (89.90(3) vs. 97.37(4)°). The distance between the Cp ring and the iron center averages 2.061(3) Å, indistinguishable from the Fe–C distance of 2.065(3) Å found in the related 9S3/Cp mixed sandwich complex and also close to the Fe–C distance of 2.064(3) Å found in ferrocene [31]. The average Fe–S length in **3** is 2.1823(7) Å compared to 2.2636(5) Å in $[Fe(10S3)_2]^{2+}$ [6]. This Fe–S bond length is particularly noteworthy as it is among the shortest Fe(II)–S(thioether) bonds known [32][1]. We believe that this large decrease for the mixed sandwich complex may be due to the enhanced iron thioether π bonding in complex **3** (relative to $[Fe(10S3)_2]^{2+}$) resulting from the presence of the σ-donating Cp ring. The iron is thus better able to π-donate to the thioether because of electronic affects associated with the Cp ligand. This structural feature of the complex is also related to our electrochemical data (see below). Viewing the cation of **3** through the 10S3 ligand, the central methylene carbon of the propylene chain is opposite a pair of adjacent carbons on the Cp ring in a staggered conformation. This conformation is approximately 8 kcal lower in energy than the eclipsed structure according to molecular mechanics calculations[2].

[1] Typical lengths for Fe(II)–S(thioether) bonds in macrocyclic complexes have been observed in the approximate range 2.24–2.34 Å. See Refs. [6,8,9,32].

[2] For our molecular mechanics study, we have used CAChe software from Oxford Molecular, Inc. The relative energies for the two conformations were: staggered: 92.99 kcal, eclipsed 85.04 kcal.

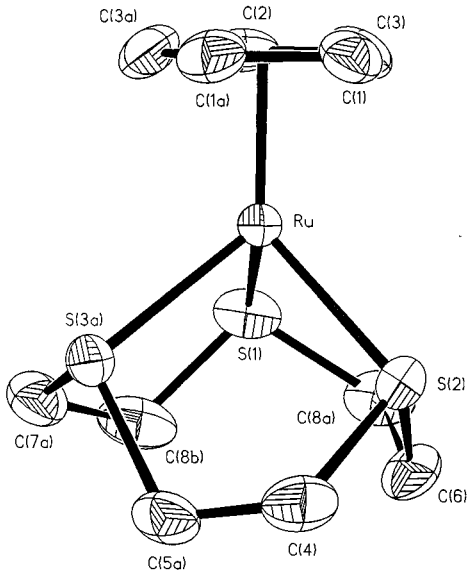

Fig. 1. Molecular structure of the cation in $[Ru(Cp)(9S3)](PF_6)$ (**1**) (50% ellipsoids, H atoms omitted). There is a disorder in the 9S3 ring resulting in two orientations related by a mirror plane. These are present in equal amounts.

In contrast to the 10S3 ligand, the lowest-energy conformation of the free 9S3 ligand has three *endodentate* sulfur atoms, and this symmetrical conformation can readily chelate to the metal center [29]. In the structure of **1** (Fig. 1), the 9S3 ligand exhibits this lowest-energy[3] conformation for tridentate complexation. The S–Ru–S chelate bond angles are compressed somewhat from the ideal with an average value of 88.10(2)°. They vary only slightly from those found in $[Ru(9S3)_2]^{2+}$ and the analogous iron(II) complex [8,11].

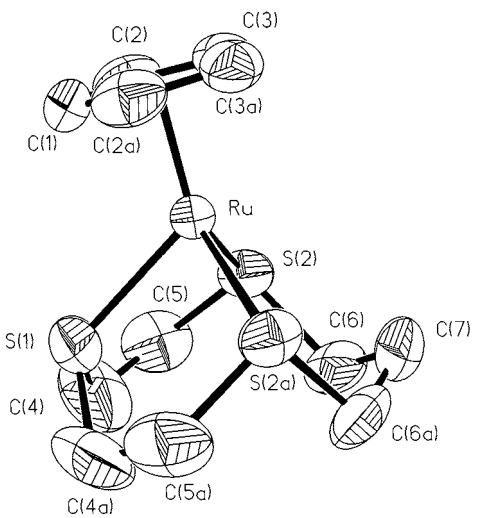

Fig. 2. Molecular structure of the cation in $[Ru(Cp)(10S3)](PF_6)$ (**2**) (50% ellipsoids, H atoms omitted). There is a disorder in the 10S3 ring resulting in three different conformers.

[3] See footnote 2.

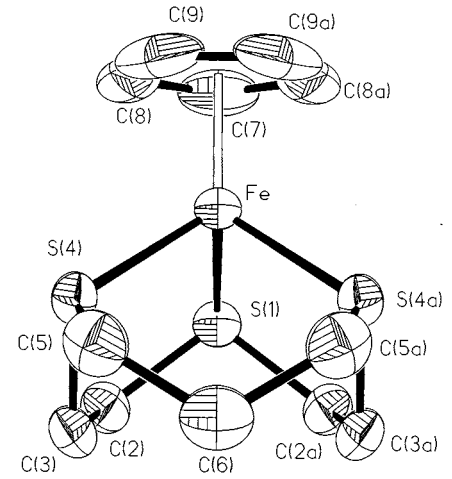

Fig. 3. Molecular structure of the cation in $[Fe(Cp)(10S3)](PF_6)$ (**3**) (50% ellipsoids, H atoms omitted. This view is along the molecule's mirror plane.

The Ru–C distances in **1** are significantly shorter than those found in ruthenocene (2.159(3) versus 2.21 Å) [33]. The Ru–S bond distances in **1** are also shorter than in the homoleptic bis 9S3 complex, 2.289(2) versus 2.339 Å [10]. The Ru–S bond distances in the two reported mixed sandwich complexes are among the shortest of this type [34][4]. Again, the presence of the σ-donating Cp ring and the enhanced metal–thioether π bonding are responsible for this decrease in the Ru–S bond length for the mixed sandwich complex. The five carbon atoms of the Cp ring lie essentially in a plane with a mean deviation from the plane of only 0.005 Å.

In the structure of **2** the Ru–C distances of the cation are slightly shorter than in ruthenocene (2.187(4) vs. 2.21 Å) and the Ru–S bond distances are also shorter than in $[Ru(10S3)_2]^{2+}$ (2.331(2) Å versus 2.342(1)Å). We feel this structural data again supports the relative σ and π donor/acceptor properties of the Cp and trithioether ligands. The S–Ru–S bond angle for the six-membered chelate ring is larger (104.10(12)°) than the corresponding angle (93.3(1)°) of the six-membered ring in the $[Ru(10S3)_2]^{2+}$ cation [12]. Commensurately, there is a 4.6° decrease in the average of the S–Ru–S bond angles for the two five-membered chelate rings (82.97(7)°). In going from the hexakis(thioether) complex to the mixed sandwich complex, the chelate bite angle for the six-membered ring has enlarged while the one for the five-membered ring has compressed. Similar relative bond angle values for five- and six-membered chelate rings have been observed in other structures involving 10S3 complexes [10,13]. As in the cation in **3**, the predominant $[Ru(Cp)(10S3)]^{+}$ conformation in the

[4] Typical lengths for Ru(II)–S(thioether) bonds in macrocyclic complexes have been observed in the approximate range of 2.23–2.44 Å. See Refs. [10–12,16,17,35].

crystal is a staggered arrangement of the central methylene of the propylene fragment of the 10S3 and the Cp ring carbons. Interestingly, the 10S3 in **2** adopts the [1324] conformation which places the six-membered chelate ring in a boat conformation [6]. To date all crystal structures of complexes involving the 10S3 ligand with first row transition metals show the ligand adopting exclusively a chair conformation as in **3**. This ligand, however, does adopt a boat conformation in the structure of $[Mo(10S3)(CO)_3]$ [26]. We suggest that the larger size of the second row transition metals could be responsible for the difference in structural behavior of the complexes.

2.3. Electrochemical studies

Cyclic voltammetry was performed on the complexes in order to compare the relative abilities of the coordinated ligands to stabilize divalent oxidation states of iron and ruthenium. The voltammograms of $[Ru(Cp)(10S3)]^+$, $[Fe(Cp)(10S3)]^+$ and $[Ru(Cp)(9S3)]^+$ all show a single oxidation wave as presented in Table 3. These oxidations are assigned as metal-centered M(II)/M(III) couples based upon the redox properties of the free ligands and the reported electrochemical behavior of the related hexakis(thioether) complexes [8–12]. No reduction or additional oxidation waves were observed.

Since the structures of $[M(Cp)L]^+$ complexes are intermediate between those of the $[ML_2]^{2+}$ and $M(Cp)_2$, it is therefore not surprising that the values for the M(II)/M(III) couples of the three mixed sandwich complexes lie intermediate between the values for the corresponding homoleptic thioether complexes and metallocenes. The ruthenium complexes are all more resistant to oxidation to the trivalent state than their iron congeners due to the enhanced π bonding between the softer Ru(II) center and the thioether ligand. As expected the presence of the thioether stabilizes the divalent state, but this stabilization is further enhanced by the replacement of the Cp ligand by a second coordinated thioether. That is, the metallocenes are oxidized most easily while the hexakis(thioether) complexes are hardest to oxidize. The size of the thioether ring also influences the redox stabilities of the complexes. The 9S3 ligand stabilizes the divalent oxidation state more effectively than does 10S3, and this observation is true for all trithioether complexes with Fe and Ru—both homoleptic and heteroleptic. We suggest that the larger and more flexible 10S3 ring size is better able to accommodate the structural changes which must accompany the oxidation of the metal due to the smaller radius of the trivalent ion.

3. Experimental

3.1. Materials

The complex $[Ru(Cp)(PPh_3)_2Cl]$ was prepared according to published procedures [30]. The compounds $[Fe(Cp)(CO)_2I]$, NH_4PF_6, 9S3 and 10S3 were purchased from Aldrich Chemical Company and used without further purification. All solvents were used as received.

3.2. Measurements

Analyses were performed by Atlantic Microlab, Atlanta, GA. ^{1}H- and $^{13}C\{^1H\}$-NMR spectra were obtained at 298K on a Varian Gemini 300 MHz NMR spectrometer using CD_3NO_2 for both the deuterium lock and reference. Carbon functionality was confirmed for all complexes by a DEPT experiment. Solution UV–vis spectra were obtained on a Varian DMS 200 UV–vis spectrophotometer. Infrared spectra were obtained using a Mattson Galaxy Series 5000 FTIR spectrometer. Cyclic voltammograms were recorded using a Princeton Applied Research Versastat Polarographic Analyzer. The electrochemistry of the two Ru complexes was studied using sample concentrations of 4 mM in CH_3NO_2 and a scan rate of 25 mV s^{-1}. The Fe complex was studied in CH_3CN with sample concentrations of 2 mM and a scan rate of 25 mV s^{-1}. In all electrochemistry experiments, the supporting electrolyte was 0.1 M Bu_4NBF_4, and the ferrocene/ferrocenium couple was used as an internal reference. The standard three-electrode configuration was as follows: Pt working electrode, Pt-wire auxiliary electrode, and Ag/AgCl reference electrode.

3.3. Preparation of [Ru(Cp)(9S3)]PF_6 (1)

A mixture of $[Ru(Cp)(PPh_3)_2Cl]$ (0.161 g, 0.222 mmol), 9S3 (0.040 g, 0.222 mmol) and 20 ml acetonitrile was refluxed under nitrogen for 18 h. The product was isolated as an orange solid by evaporation of solvent. The PF_6^- salt was precipitated by addition of NH_4PF_6 (0.041 g, 0.25 mmol) to the orange chloride salt in 20 ml of methanol. The $[Ru(Cp)(9S3)]PF_6$ product was dissolved in nitromethane and recrystallized by the slow addition of ether. Yield: 0.045 g (41%). ^{13}C-NMR (CD_3NO_2): δ 79.4 (Cp), 36.2 ppm (9S3). ^{1}H-NMR (CD_3NO_2): δ 4.83 (s, Cp, 5 H), 3.2 to 2.5 ppm (ABCD pattern, 9S3, 12 H). IR (KBr): 3125, 3017, 2974, 2938, 1448, 1413, 1290, 1171, 1104, 1014, 948, 910, 836 (s, PF_6^-), 675 cm^{-1}. Anal. Calc. for $C_{11}H_{17}F_6PRuS_3$: C, 26.88; H, 3.49; S, 19.57%. Anal. Found: C, 27.12; H, 3.43; S, 19.29%. UV–vis (CH_3CN): λ_{max} 313 nm ($\varepsilon = 862$ M^{-1} cm^{-1}), 304 (1418).

3.4. Preparation of [Ru(Cp)(10S3)]PF_6 (2)

A mixture of [Ru(Cp)(PPh_3)$_2$Cl] (0.349 g, 0.481 mmol) and 10S3 (0.093 g, 0.481 mmol) was refluxed in 40 ml of acetonitrile for 4 days. The solvent was evaporated, and the product was redissolved in 20 ml of methanol. Any undissolved solid was removed by filtration, and excess NH_4PF_6 (0.081 g, 0.50 mmol) was added to the filtrate to precipitate the complex as the PF_6^- salt. Yellow–brown crystals were isolated by recrystallization of the crude product from nitromethane/ether (Scheme 1). Yield: 0.061 g (25%). ^{13}C-NMR (CD_3NO_2): δ 79.5 (Cp), 38.1, 37.0, 31.7, 25.2 ppm (10S3). ^{1}H-NMR (CD_3NO_2): δ 4.85 (Cp, 5 H), 3.4 to 2.4 ppm (10S3 broad, complex resonances, 14 H). IR (KBr,): 3140, 3057, 2963, 2926, 1481, 1437, 1275, 1183, 1120, 1029, 917, 839 (s, PF_6^-) 684 cm^{-1}. Anal. Calc. for $C_{12}H_{19}F_6PRuS_3$: C, 28.51; H, 3.79; S, 19.03%. Anal. Found: C, 28.79; H, 3.72; S, 18.78%. UV–vis (CH_3CN): λ_{max} 314 nm ($\varepsilon = 860$ M^{-1} cm^{-1}), 305 (1006), 255 (59).

3.5. Preparation of [Fe(Cp)(10S3)]PF_6 (3)

A solution of [Fe(Cp)(CO)$_2$I] (0.391 g, 1.29 mmol), 10S3 (0.250 g, 1.29 mmol) and 25 ml acetonitrile was refluxed under nitrogen for 18 h. Solvent was removed under vacuum. The solid was dissolved in 10 ml methanol and precipitated as the PF_6^- salt by the addition of excess NH_4PF_6 (0.30 g, 1.8 mmol) to the solution. The brick-red crystals were filtered and washed with 15 ml ether and air-dried (Scheme 1). Yield: 0.543 g (92%). Crystals suitable for X-ray diffraction were obtained by diffusion of ether into a nitromethane solution. ^{13}C-NMR (CD_3NO_2): δ 77.2 (Cp), 39.5, 37.5, 30.2, 20.5 ppm (10S3). ^{1}H-NMR (CD_3NO_2): δ 4.53 (Cp, 5 H), 3.0–1.7 ppm (10S3 broad, complex resonances, 14 H). IR (KBr): 3120, 2962, 2926, 1449, 1425, 1298, 1186, 1110, 1020, 947, 911, 837 (PF_6^-), 668 cm^{-1}. Anal. Calc. for $C_{12}H_{19}F_6FePS_3$: C, 31.31; H, 4.16; S, 20.90%. Anal. Found: C, 31.38; H, 4.17; S, 20.76%. UV–vis (CH_3CN): λ_{max} 470 nm ($\varepsilon = 31$ M^{-1} cm^{-1}), 301 (1359), 268 (7450).

3.6. X-ray structural analysis

X-ray diffraction data were collected on a Siemens R3m/V automated diffractometer fitted with a molybdenum source and a graphite monochromator ($\lambda = K_\alpha = 0.71073$ Å). Structures were determined using direct methods (SHELXS-86) [35] and refined by full-matrix least-squares methods (SHELXL-93) [36]. Hydrogen atom positions on carbons in the crown thioether ligands were assigned idealized locations. In the Fe(II) complex, these atoms were included in structure factor calculations but not refined. In the Ru(II) complexes, the coordinates were refined but not the s.o.f. or U(eq) values. A semi-empirical absorption correction was determined and applied to the data [37]. Scattering factors were taken from International Tables for X-ray Crystallography. The crystal data and experimental parameters for all three structures are reported in Table 1.

3.6.1. X-ray crystal structure of [Ru(Cp)(9S3)]PF_6 (1)

A clear yellow crystal with dimensions 0.07 × 0.05 × 0.10 mm was selected for data collection. Automatic peak search and indexing procedures yielded a c-centered monoclinic cell. Inspection of the Niggli values revealed no conventional cell of higher symmetry. Data was collected using omega scans (1°, 1°) from $3.5° < 2\theta < 56°$ with only data $I \geq 2\sigma(I)$ considered observed. Hydrogen atom positions on carbons on the cyclopentadienyl ring were located in the difference maps with the coordinates refined but s.o.f. or U(eq) values unrefined. The final R was 0.0298 for 143 variables, $wR^2 = 0.0791$, goodness-of-fit = 1.235. The final difference features did not exceed +1.061 and −0.846 e Å^{-3}. Selected bond lengths and angles are given in Table 2.

3.6.2. X-ray crystal structure of [Ru(Cp)(10S3)]PF_6 (2)

A clear yellow crystal with dimensions 0.05 × 0.05 × 0.03 mm was selected for data collection. Automatic peak search and indexing procedures yielded a c-centered monoclinic cell. Inspection of the Niggli values revealed no conventional cell of higher symmetry. Data was collected using omega scans (1°, 1°) from $3.5° < 2\theta < 65°$ with only data $I \geq 2\sigma(I)$ considered observed. Hydrogen atom positions on carbons on the cyclopentadienyl ring were located in the difference maps with the coordinates but not the s.o.f. or U(eq) values refined. The final R was 0.0526 for 131 variable, $wR^2 = 0.1362$, goodness-of-fit = 0.953. The final difference features did not exceed +2.517 and −1.621 e Å^{-3}. Selected bond lengths and angles are given in Table 2.

3.6.3. X-ray crystal structure of [Fe(Cp)(10S3)]PF_6 (3)

A clear red crystal with dimensions 0.5 × 0.2 × 0.1 mm was selected for data collection. Automatic peak search and indexing procedures yielded a monoclinic reduced primitive cell. Inspection of the Niggli values revealed no conventional cell of higher symmetry. Data was collected using omega scans (1°, 1°) from $3.5° < 2\theta < 60°$ with only data $I \geq 2\sigma(I)$ considered observed. The final R was 0.0394 for 218 variables, $wR^2 = 0.1128$, goodness-of-fit = 0.924. The final difference features did not exceed +0.707 and −0.475 e Å^{-3}. Selected bond lengths and angles are given Table 2.

Table 2
Selected bond lengths (Å) and bond angles (°) with S.D. [a]

[CpRu(9S3)][PF_6]			
Bond lengths (Å)			
Ru–S(3)	2.288(2)	S(3)–C(4)	1.813(11)
Ru–S(1)	2.256(2)	S(1)–C(6)	1.835(8)
Ru–S(2)	2.323(2)	S(1)–C(1)	1.856(4)
Ru–C(9)	2.189(3)	S(2)–C(2)	1.805(7)
Ru–C(7)	2.125(4)	S(2)–C(3)	1.814(13)
Ru–C(8)	2.157(3)	C(6)–C(5)	1.488(8)
S(3)–C(5)	1.843(14)	C(1)–C(2)	1.442(8)
		C(3)–C(4)	1.526(15)
Bond angles (°)			
S(1)–Ru–S(3)	89.18(8)	C(2)–S(2)–Ru	104.7(2)
S(2)–Ru–S(3)	86.73(10)	C(3)–S(2)–Ru	103.4(4)
S(1)–Ru–S(2)	88.39(8)	C(2)–S(2)–C(3)	100.5(5)
C(5)–S(3)–Ru	101.8(4)	C(6)–C(5)–S(3)	112.3(7)
C(4)–S(3)–Ru	108.4(3)	C(5)–C(6)–S(1)	112.7(6)
C(4)–S(3)–C(5)	103.1(6)	C(2)–C(1)–S(1)	113.6(4)
C(6)–S(1)–Ru	105.8(3)	C(1)–C(2)–S(2)	112.5(4)
C(1)–S(1)–Ru	102.55(13)	C(4)–C(3)–S(2)	113.1(10)
C(1)–S(1)–C(6)	100.2(3)	C(3)–C(4)–S(3)	110.4(8)
[Ru(Cp)(10S3)][PF_6]			
Bond lengths (Å)			
Ru–C(1)	2.171(6)	S(1)–C(4)	1.811(7)
Ru–C(2)	2.188(4)	S(2)–C(5)	1.800(7)
Ru–C(2a)	2.188(4)	S(1)–C(4a)	1.811(7)
Ru–C(3a)	2.201(4)	S(2)–C(8)	1.324(11)
Ru–C(3)	2.201(4)	S(2)–C(6)	1.854(10)
Ru–S(1)	2.302(2)	C(4)–C(5)	1.446(10)
Ru–S(2)	2.346(2)	C(6)–C(7)	1.483(14)
Ru–S(3a)	2.286(2)	S(3)–C(8)	1.823(12)
Ru–S(3)	2.286(2)	S(3)–C(7)	1.835(6)
Ru–S(2a)	2.346(2)	C(7)–C(6a)	1.483(14)
Bond angles (°)			
S(1)–Ru–S(2)	82.97(7)	C(5)–S(2)–Ru	108.4(2)
S(2a)–Ru–S(2)	104.10(12)	C(6)–S(2)–Ru	106.4(4)
C(4a)–S(1)–C(4)	104.0(6)	C(5)–C(4)–S(1)	115.1(4)
C(4)–S(1)–Ru	111.2(2)	C(4)–C(5)–S(2)	115.4(4)
C(5)–S(2)–C(6)	99.5(5)	C(7)–C(6)–S(2)	109.9(6)
S(3a)–Ru–S(1)	99.45(8)	C(6)–C(7)–C(6a)	105.5(10)
S(3)–Ru–S(2a)	86.49(12)	S(2a)–Ru–S(2)	104.10(12)
[CpFe10S3)][PF_6]			
Bond lengths (Å)			
Fe–S(l)	2.127(10)	S(l)–C(2)	1.831(3)
Fe–S(4)	2.2100(7)	S(4)–C(5)	1.818(3)
Fe–C(7)	2.069(4)	S(4)–C(3)	1.821(3)
Fe–C(8)	2.071(3)	C(3)–C(2)	1.509(4)
Fe–C(9)	2.048(3)	C(5)–C(6)	1.514(4)
Bond angles (°)			
S(4a)–Fe–S(4)	97.37(4)	C(5)–S(4)–Fe	112.51(10)
S(4)–Fe–S(1)	89.90(3)	C(3)–S(4)–Fe	106.15(9)
C(2a)–S(l)–C(2)	103.4(2)	C(2)–C(3)–S(4)	108.8(2)
C(2)–S(l)–Fe	104.65(9)	C(3)–C(2)–S(1)	113.7(2)
C(5)–S(4)–C(3)	101.91(13)	C(6)–C(5)–S(4)	117.5(2)
		C(5)–C(6)–C(5a)	116.5(3)

[a] Symmetry transformations used to generate equivalent atoms: for [CpRu(9S3)][PF_6] (a) or (b) $x, -y+1/2, z$ (c) $-x-1, -y, -z+1$; for [Ru(Cp)(10S3)][PF_6] (a) $x, -y+1/2, z$ (b) $-x+1, -y, -z+1$; and for [CpFe(10S3)][PF_6] (a) $x, -y+1/2, z$ (b) $-x+1, -y, -z+1$.

Table 3
Electrochemical data for Fe(II) and Ru(II) trithioether complexes

	$E_{1/2}$ (mV) [a]	
	L = 9S3	L = 10S3
$[Ru(Cp)L]^+$	+966 (irrev.) [b]	+764 (quasi-rev.) [b]
$[Fe(Cp)L]^+$	+440 (rev) [c] [20]	+305 (rev.) [d]
$[Ru(L)_2]^{2+}$	+1410 (quasi-rev.) [11]	+1370 (quasi-rev.) [12]
$[Fe(L)_2]^{2+}$	+982 (rev.) [8]	+910 (rev) [9]

[a] Formal M(II)/M(III) redox potentials in volts measured vs. ferrocene/ferrocenium ($Fc/Fc^+ = 0$ mV). For comparison the Ru(II)/Ru(III) couple for ruthenocene occurs at +265 mV under our experimental conditions.

[b] This work; measured in CH_3NO_2.

[c] We observe this couple at +437 mV, essentially the same value as the reported one.

[d] This work; measured in CH_3CN.

4. Conclusions

Heteroleptic sandwich complexes of Ru(II) and Fe(II) with C_5H_5 and the trithioethers 9S3 and 10S3 can be readily prepared. The structures of the three reported complexes all show an octahedral metal center with facially coordinating Cp and crown trithioether ligands. The spectroscopic, electrochemical, and structural properties of the complexes can be explained by the strong σ-donating ability of the Cp ligand and the effect that it has on the π bonding between the metal ion and the trithioether. The behavior of these mixed sandwich complexes lies between the analogous metallocene and homoleptic hexakis(thioether) complexes.

5. Supplementary material

Complete listings for $[Ru(C_5H_5)(9S3)]PF_6$, $[Ru(C_5H_5)(10S3)]PF_6$, and $[Fe(C_5H_5)(10S3)]PF_6$: crystallographic data, (5 pages), atomic coordinates (3 pages), bonding distances and angles (7 pages), anisotropic thermal parameters (3 pages) and hydrogen atom coordinates (3 pages) are all available from the author.

Acknowledgements

This research was generously supported by grants from the Research Corporation, the National Science Foundation (RUI Program), and the Grote Chemistry Fund at UTC. One of us (T.S.B.) would like to thank

the Camille and Henry Dreyfus Foundation for a post-doctoral fellowship through their Scholar/Fellow Program at Undergraduate Institutions. The support of the National Science Foundation ILI Program is also acknowledged for the purchase of a Gemini 300 MHz NMR Spectrometer. We also appreciate the assistance of Chris Brandow (UTC) for help with some of the NMR measurements and Professor Bill Pennington (Clemson University) for his beneficial comments in the preparation of the manuscript.

References

[1] A.J. Blake, M. Schröder, in: A.G. Sykes (Ed.), Advances in Inorganic Chemistry, Academic Press, New York, 1990, p. 2.
[2] S.R. Cooper, Acc. Chem. Res. 21 (1988) 141.
[3] S.R. Cooper, S.C. Rawle, Struct. Bonding Ber. 72 (1990) 1.
[4] M. Schröder, Pure Appl. Chem. 60 (1988) 517.
[5] S.G. Murray, F.R. Hartley, Chem. Rev. 81 (1981) 365.
[6] W.N. Setzer, E.L. Cacioppo, Q. Guo, G.J. Grant, D.D. Kim, J.L. Hubbard, D.G. VanDerveer, Inorg. Chem. 29 (1990) 2672.
[7] M.N. Bell, A.J. Blake, M. Schröder, H.-J. Kuppers, K. Wieghardt, Angew. Chem. Int. Ed. Engl. 26 (1987) 250.
[8] K. Wieghardt, H.-J. Küppers, J. Weiss, Inorg. Chem. 24 (1985) 3067.
[9] G.J. Grant, S.M. Isaac, W.N. Setzer, D.G. VanDerveer, Inorg. Chem. 32 (1993) 4284.
[10] S.C. Rawle, T.J. Sewell, S.R. Cooper, Inorg. Chem. 26 (1987) 3769.
[11] S.C. Rawle, S.R. Cooper, J. Chem. Soc. Chem. Commum. (1987) 308.
[12] G.J. Grant, B.M. McCosar, W.N. Setzer, J.D. Zubkowski, E.J. Valente, L.F. Mehne, Inorg. Chim. Acta 244 (1996) 73.
[13] S. Chandrasekhar, A. McAuley, Inorg. Chem. 31 (1992) 480.
[14] R.D. Adams, S.B. Falloon, K.T. McBride, J.H. Yamamoto, Organometallics 14 (1995) 1739.
[15] R.D. Adams, J.H. Yamamoto, Organometallics 14 (1995) 3704.
[16] M.A. Bennett, L.Y. Goh, A.C. Willis, J. Am. Chem. Soc. 118 (1996) 4984.
[17] A.J. Welch, A.S. Weller, Inorg. Chem. 35 (1996) 4548.
[18] K. Brandt, W.S. Sheldrick, J. Chem. Soc. Dalton Trans. (1996) 1237.
[19] J. Cannadine, A. Hector, A.F. Hill, Organometallics 11 (1992) 2333.
[20] A.J. Blake, M.A. Halcrow, M. Schröder, J. Chem. Soc. Chem. Commun. (1991) 253.
[21] A.J. Blake, R.D. Crofts, G. Reid, M. Schröder, J. Organomet. Chem. 359 (1989) 371.
[22] H-J. Kim, J-H. Lee, I-H. Suh, Y. Do, Inorg. Chem. 34 (1995) 796.
[23] M.N. Bell, A.J. Blake, R.M. Christie, R.O. Gould, A.J. Holder, T.I Hyde, M. Schröder, L.J. Yellowlees, J. Chem. Soc. Dalton Trans. (1992) 2977.
[24] A.J. Blake, M.A. Halcrow, M. Schröder, J. Chem. Soc. Dalton Trans. (1994) 1631.
[25] M.A. Bennett, L.Y. Goh, A.C. Willis, J. Chem. Soc. Chem. Commun. (1992) 1180.
[26] G.J. Grant, J.P. Carpenter, W.N. Setzer, D.G. VanDerveer, Inorg. Chem. 28 (1989) 4128.
[27] M.T. Ashby, D.L. Lichtenberger, Inorg. Chem. 24 (1985) 636.
[28] H.J. Kim, Y. Do, H.W. Lee, J.H. Jeong, Y.S. Sohn, Bull. Kor. Chem. Soc. 12 (1991) 257.
[29] R.S. Glass, G.S. Wilson, W.N. Setzer, J. Am. Chem. Soc. 102 (1980) 5068.
[30] L. Ballester, A. Gutierrez, M.F. Perpinan, J. Chem. Ed. 66 (1989) 777.
[31] C.M. Lukehart, Fundamental Transition Metal Organometallic Chemistry, Brooks/Cole, Monterey, CA, 1985, p. 90.
[32] (a) U. Heinzel, A. Henke, R. Mattes, J. Chem. Soc. Dalton Trans. (1997) 501. (b) H.-J. Küppers, K. Wieghardt, B. Nuber, J. Weiss, E. Bill, A.X. Trautwein, Inorg. Chem. 26 (1987) 3762. (c) J.P. Danks, N.R. Champness, M. Schröder, Coord. Chem. Rev. 174 (1998) 417. (d) G. Reid, M. Schröder, Chem. Soc. Rev. 19 (1990) 239.
[33] C. Elschenbroich, A. Salzer, Organometallics: A Concise Introduction, VCH, New York, 1992, p. 323.
[34] (a) D.P. Riley, J.D. Oliver Inorg. Chem, 25 (1986) 1814. (b) D.P. Riley, J.D. Oliver, Inorg. Chem. 25 (1986) 1821. (c) W.A. Schenk, J. Frisch, M. Dürr; N. Burzlaff, D. Stalke, R. Fleischer, W. Adam, F. Prechtl, A. Smerz, Inorg. Chem 36 (1997) 2372. (d) C. Landgrafe, W. Sheldrick, J. Chem. Soc. Dalton Trans. (1994) 1885. (e) M.A. Bennett, L.Y. Goh, A.C. Willis, J. Chem. Soc. Chem. Commun. (1992) 1180. (f) J.C. Cannadine, A.F. Hill, A.J.P. White, D.J. Williams, J.D.E.T. Wilton-Ely, Organometallics 15 (1996) 5409. (g) A.J. Blake, R.M. Christie, Y.V. Roberts, M.J. Sullivan, M. Schröder, L.J. Yellowlees, J. Chem. Soc. Chem. Commun. (1992) 848. (h) M.N. Bell, A.J. Blake, A.J. Holder, T.I. Hyde, M. Schröder, J. Chem. Soc. Dalton Trans. (1990) 3841. (h) M.N. Bell, A.J. Blake, M. Schröder, H.-J. Kuppers, K. Wiedghardt, Angew. Chem. Int. Ed. Engl. 26 (1987) 250. (i) M.A. Bennett, A.C. Willis, L.Y. Goh, W. Chen, Polyhedron 15 (1996) 3559. (j) B.J. Goodfellow, V. Felix, S.M.D. Pacheco, J.P. de Jesus, M.G.B. Drew, Polyhedron 16 (1996) 393. (k) D. Sellmann, H.-P. Neuner, R. Eberlein, M. Moll, F. Knock, Inorg. Chim. Acta 175(1990) 231.
[35] G.M. Sheldrick, Acta Crystallogr. A46 (1990) 467–473.
[36] G.M. Sheldrick, SHELX-93: Program for Crystal Structure Refinement, Göttingen University, Göttingen, Germany, 1993.
[37] SHELXA-90, ver. 1, Siemens Analytical X-Ray Instruments, Madison, WI, 1990.